Studies on Fly Ash–Filled Epoxy-Cast Slabs Under Compression

S. M. KULKARNI, KISHORE

Polymer Composites Laboratory, Metallurgy Department, Indian Institute of Science, Bangalore 560 012, India

Received 15 July 2001; accepted 18 August 2001

ABSTRACT: Filling a polymer with particulate material is generally attempted to improve the polymer properties and also realize some reduction in the cost. In the present work, we attempted to study the viability of using fly ash, an industrial waste with good mechanical properties, as a filler in epoxy. Initial low volumes of filler display an improvement in compressive strength and modulus. The experimental values of strength and modulus are also found to correlate well with those predicted by the rule of mixtures and modified Kerner's equation. At higher volume fractions, the decline in these properties is explained in the context of both percolation theory and Griffith's theory. The processes of failure initiation and propagation proposed are examined from the viewpoint of observations on the surfaces of compression-failed samples in SEM. © 2002 Wiley Periodicals, Inc. J Appl Polym Sci 84: 2404–2410, 2002

Key words: epoxy; fly ash; compression properties; SEM

INTRODUCTION

Polymers are generally filled with particulate material to improve their mechanical, thermal, or rheological properties. A secondary benefit arising out of this is the reduction in the total cost of the composite. Toward this end it is natural to look for a very cheap and abundantly available material as filler. Materials such as minerals and inorganic oxides, such as alumina and silica and other cheaper ones such as chalk and sand, are mixed into widely employed thermoplastic materials such as polypropylene[1–7] and polyethylene.[8,9] Very little attention is focused on filler-bearing thermosets in general and epoxies in particular where the fillers belong to the above-mentioned mineral matter[10] and inorganic oxide[11] varieties.

Fly ash, a fine powder generated in large amounts during the combustion of coal in thermal power plants with its good mechanical properties is a candidate material for being used as filler. This low-cost filler was used in some earlier studies with different polymer matrices such as polyester,[12,13] polypropylene,[14] and epoxy[15] to study the mechanical properties in tension and impact. The behavior pattern under compression, however, has not been looked into and hence the present study. The fly ash used consists of small spherical solid and hollow aluminosilicate particles (cenospheres),[16] with characteristic bimodal particle size variation. Compression tests were done in a specially designed fixture to ensure axiality of the load during testing of coupons cut from cast slabs. Modulus values obtained experimentally were compared with those obtained by two models: (1) the rule of mixtures and (2) modified Kerner's equation.[17] With regard to compression strength, the experimental values were compared to those obtained by a model based on

Correspondence to: Kishore (balkis@metalrg.iisc.ernet.in)

Journal of Applied Polymer Science, Vol. 84, 2404–2410 (2002)

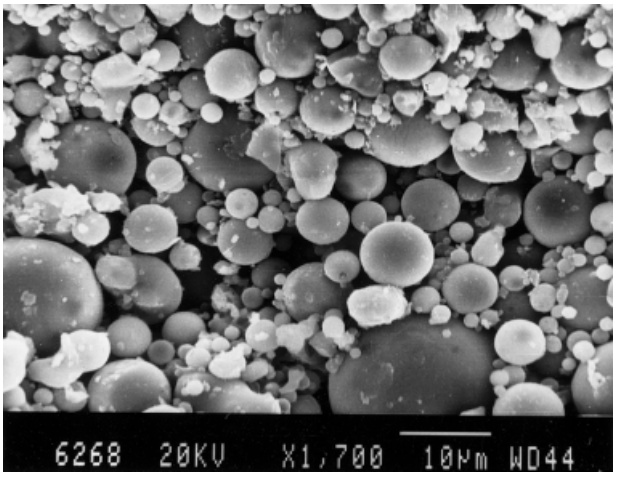

Figure 1 SEM micrograph showing assorted sizes of fly ash particles.

breaking strength (BS model),[18] a recent addition to the few models available for predicting the effective strength of the composite. Furthermore, the influence of particle distribution and particle–matrix bonding on the strength and modulus values were analyzed with reference to percolation theory[19] and Griffith's theory,[7] respectively. The deductions from such analyses were verified with observations made on the surfaces of samples fractured as a result of compression loading, employing a scanning electron microscope (SEM).

EXPERIMENTAL

Materials

The matrix system consisted of a medium viscosity epoxy resin (LAPOX L-12) and a room-temperature curing hardener with a tetraamine functional group (K-6) supplied by ATUL India Ltd. The density of cured neat resin was found to be 1.12 g/cm^3. The filler used (i.e., fly ash) was acquired from Neyveli Lignite Corp. (Neyveli, India). This ASTM class C fly ash, with bulk density of about 0.9 g/cm^3, was found to consist of a mixture of solid and hollow spheres of different sizes (Fig. 1). Particle size distribution of this fly ash, as determined by a laser light particle size analyzer (Malvern Instruments), is shown in Figure 2. This distribution typically consists of two distinct clusters characterized by a gross bimodal nature in the particle distribution (Fig. 2). One of the clusters has a distribution having a mean size of 35 μm, whereas the other is about 0.35 μm. Whereas 73% of the particles constitutes the larger-size group, the remaining 27% contains the lower average size particles. According to the bimodal theory of sphere–sphere packing, a distribution of the above nature should yield a value close to the maximum packing. Theoretical maximum packing is obtained for such sphere–sphere packing at about 72% of larger spheres and 28% of smaller spheres, when the sphere diameter ratio R tends to infinity. In the present case, with $R \geq 100$, the above-mentioned proportion of larger to smaller particles yields a packing fraction of about 82% against the value of 85%, which is the maximum theoretically attainable.[20] Finally, with regard to the compositional aspect, the energy-dispersive spectroscopy of the fly ash sample revealed the main constituents to be silica and alumina of about 63 and 26%, respectively. Other oxides present were Fe_2O_3 (7%) and TiO_2 (2.5%).

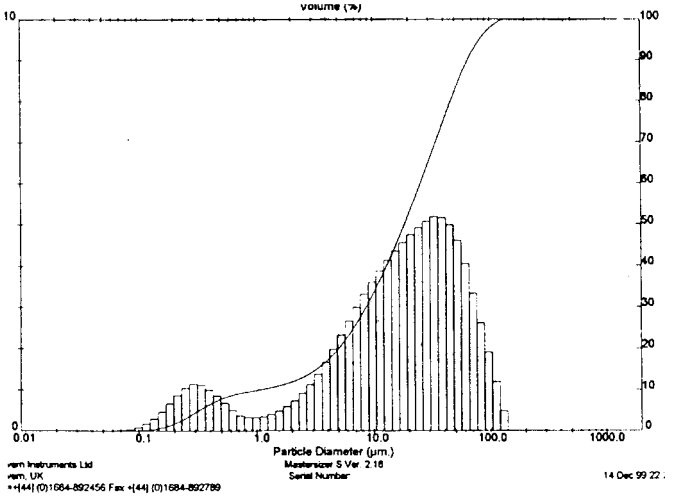

Figure 2 Particle size distribution of fly ash.

Table I Density and Void Content of Fly Ash/ Epoxy Particulate Composites

Filler (vol %)	Density (kg/m^3)	Voids (%)
(EP) 0	1120	1.7
10	1230	2.4
20	1280	7.7
25	1330	8.6
30	1370	9.9

Fabrication Procedure

A measured quantity of epoxy resin was mixed with a preweighed amount of fly ash and the hardener was added to this with gentle stirring to avoid formation of air bubbles. The mixture was then slowly decanted into a mold of size 320 × 170 × 3 mm, coated beforehand with a uniform film of silicone-releasing agent. The mixture that was like dough in the case of high-volume fractions of filler was gently spread to fill the entire mold. The mixture was left to cure at room temperature for about 24–26 h. Subsequently, postcuring was done at a temperature of 75°C for 1.5–2 h. The cured rigid plate sample was withdrawn from the mold and the edges were trimmed. The density of each sample was measured and, subsequently, an assessment of the void content was made. Table I shows these values for different volume fractions of the filler. Samples were then subjected to a C-scan nondestructive test to map out the regions of uniform material distribution from where the test coupons of required size were then sectioned from the cast slabs.

Testing

Compression testing was done in a DARTEC 9500, a servohydraulic computer-controlled testing machine. Test coupons of size 12.5 × 12.5 × 3 mm, conforming to ASTM D695M specifications, were used for compression testing. To reduce the chances of off-axial loading and the resulting slippage of the specimen, test coupons were held in a specially designed fixture. The machine crosshead was programmed to apply the compression load at a constant strain rate of 0.01 s^{-1} throughout the duration of the test. From the load–stroke history of the test provided by the machine, the compressive moduli and strength were determined.

Microscopy

Samples subjected to compression were examined by a JSM 840A SEM (JEOL, Peabody, MA). The samples were gold coated beforehand under vacuum with an ionizing current of 10 mA in an ion-sputtering unit to render them conductive.

RESULTS AND DISCUSSION

In Figures 3 and 4 compression moduli and strength values are plotted with respect to relative packing volume (i.e., the ratio of volume fraction and maximum packing density for the bimodal size distribution shown in Fig. 2). Moduli values show an increasing trend (Fig. 3), except for the last case, that is, where the relative packing volume is highest (0.36). Also superimposed in the same figure are the theoretical predictions of the modulus by two models, that is, the series model rule of mixtures, expressed mathematically as

$$E_c = \frac{E_m E_f}{E_m \nu_f + E_f \nu_m} \tag{1}$$

where E_c, E_m, and E_f are the moduli of composite, matrix, and filler, respectively; and v_m and v_f are the volume fractions of the matrix and filler, respectively.

The second model, the modified Kerner's equation,[19] is given by

$$\frac{E_c}{E_m} = \frac{AB\nu_f}{1 - B\ \psi\nu_f} \tag{2}$$

where $A = k_E - 1$ (k_E is the Einstein coefficient) and

$$B = \frac{(E_f/E_m) - 1}{(E_f/E_m + A} \text{ and } \psi = 1 + \left(\frac{1 - P_f}{P_f^2}\right)\nu_f \tag{3}$$

where P_f corresponds to the packing fraction of the filler at maximum concentration.

It can be noticed in the plot that series model values in general match well with experimental values falling in the scatter band (Fig. 3). However, the values based on the modified Kerner's equation predictions lie on the higher side as a result of the intrinsic assumption of good binding at the fiber–matrix interface. The series model, on

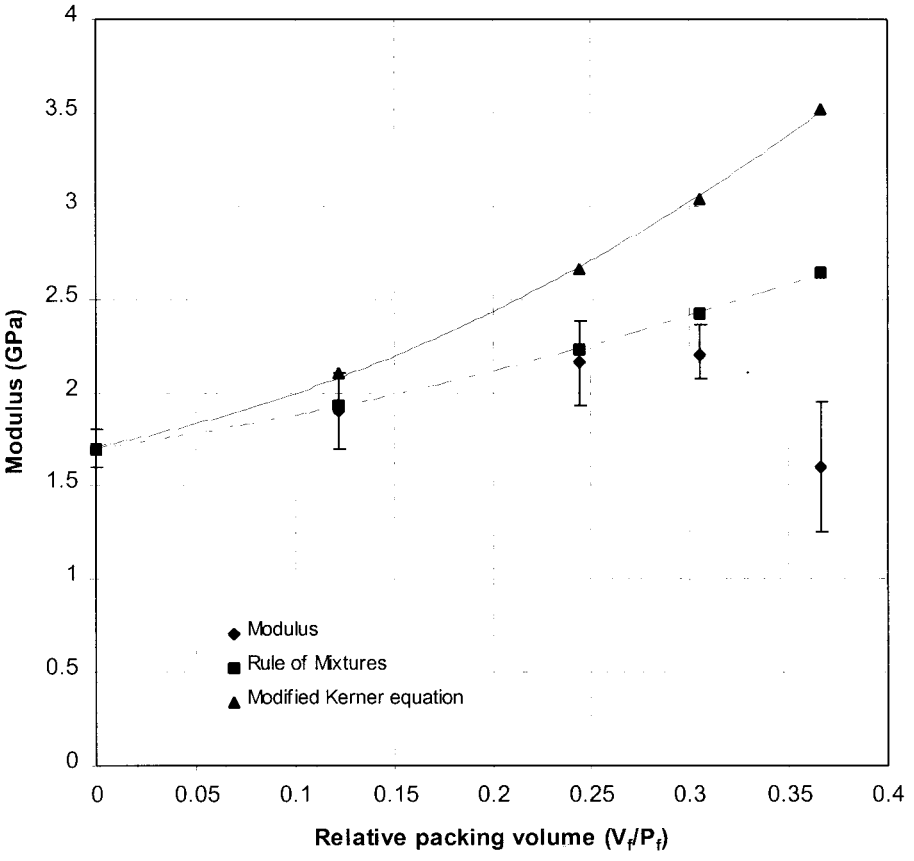

Figure 3 Variation of modulus with relative packing volume.

the other hand, which assumes no bonding at the interface, yields values closer to the experimental results. It can also be noted that the increase in the modulus between relative packing volumes 0.12 and 0.24 is greater than that noticed between 0.24 and 0.3 (Fig. 3). To explain this behavior, we resorted to the percolation model in this work, as detailed below.

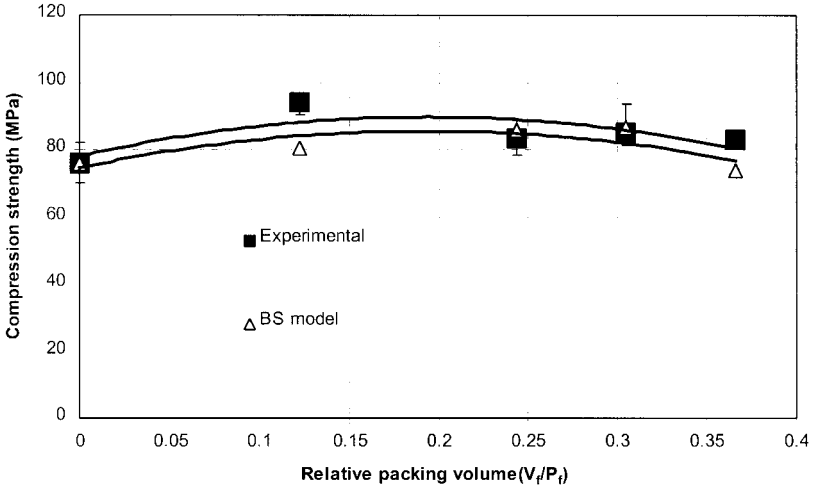

Figure 4 Plot showing the variation compressive strength with relative packing volume.

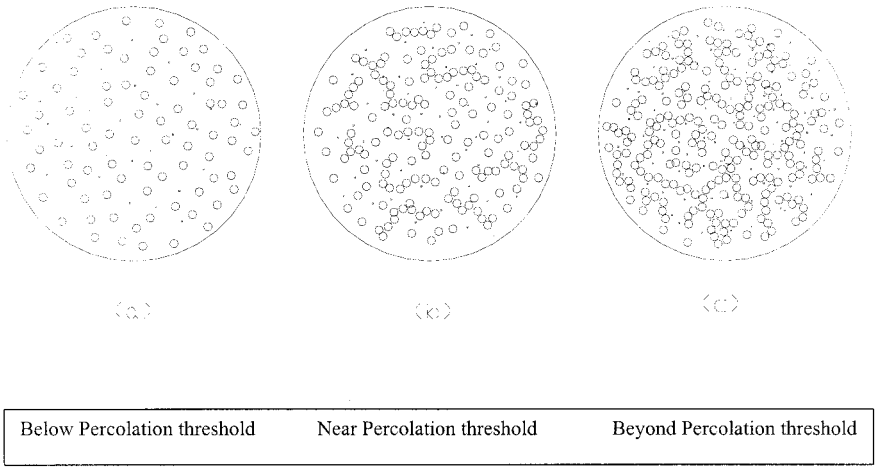

Figure 5 Schematic showing the particle distribution and formation of percolation pathways near threshold levels of filler material.

In the composite, when the filler particles are packed randomly they tend to form interconnected networks, called *percolation pathways* (Fig. 5), beyond a critical volume fraction or threshold.[19] The stress fields around filler particles, attributed to differences in moduli of the matrix and the filler,[21] interact when the volume fraction is near threshold and cause a significant behavioral change in the composite. For the present case, with bimodal packing of fly ash particles, the percolation threshold (~ 0.196) is very close to the volume fraction of 0.2 (corresponding to the relative packing volume of 0.24). Beyond this volume fraction, for the fly ash particles that are partially bonded to the matrix, given the inability of resin to smear the particles' surface completely because of clustering of particulates, display what may be called *debonded regions* (Fig. 6), which later during compression act as crack initiators (Figs. 7 and 8). Such cracks that originated around particles tend to join to yield place to a major crack when the interparticle distances at higher volume fractions are less (Fig. 9). These conditions favor early failure of the composite, with a resulting reduction in strength and modulus.

It can be noticed in Figure 4 that strength initially increases but beyond a relative packing volume of 0.12, it decreases. This initial increase is attributed to the crack-pinning effect by the filler particles.[15] Also, at this lower concentration, particles are less prone to form a network [Fig. 5(a)] and the resulting larger interparticle distances do not allow the stress volumes (mentioned previously)[21] around the particles to interact; hence, the strengthening effect can be seen. When the volume fraction is increased, the particles tend to come closer and form percolation pathways, with resulting interactions of the stress fields around the particles causing reduction in strength, as stated earlier.

Theoretical strength values predicted by the breaking strength (BS) model[18] are plotted in Figure 4. These compare well within the scatter and also follow the same trend with respect to the volume fraction as those of experimental results. As emphasized before, the fly ash used characteristically consists of a bimodal particle size distribution (Fig. 2), in which larger particle surfaces demonstrate a lower propensity to adhesion by the matrix. By applying Griffith's theory to the

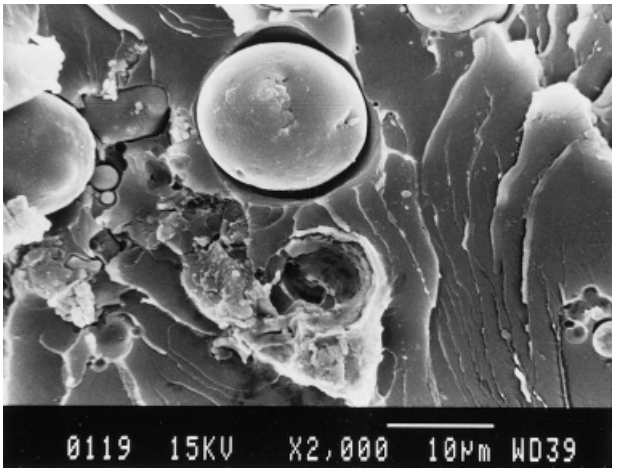

Figure 6 SEM micrograph displaying the clear debonds at the interface of larger-size particles.

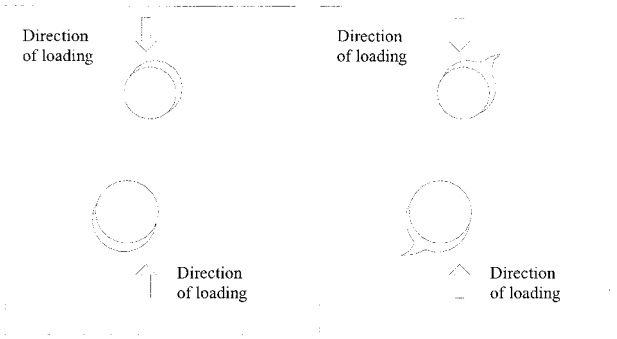

Figure 7 Schematic showing the initiation of crack at the debonds of filler–matrix regions.

formation of a dewetting cavity, it is noted that the stress for dewetting is inversely proportional to the square of particle radius.[7] Thus at larger particle surfaces, the tendency to dewet exists, unlike in smaller particles where the stress required for formation of a dewetting cavity is significant. Figure 10 shows large crescent-shape debonds at the filler particle surface resulting from dewetting. In the same micrograph the lesser tendency for debonds to form at interfaces of matrix and smaller particles (indicated by arrows Fig. 10) can also be noted.

This debond aids the formation of crack because of the opening mode tensile fracture at the inner surfaces of the dewetting cavities (Fig. 7). At higher concentrations of the filler, when the interparticle distances are small, these cracks originating at the debond (Fig. 11) join, thus favoring an early failure of the composite and attendant decrease in both strength and modulus,

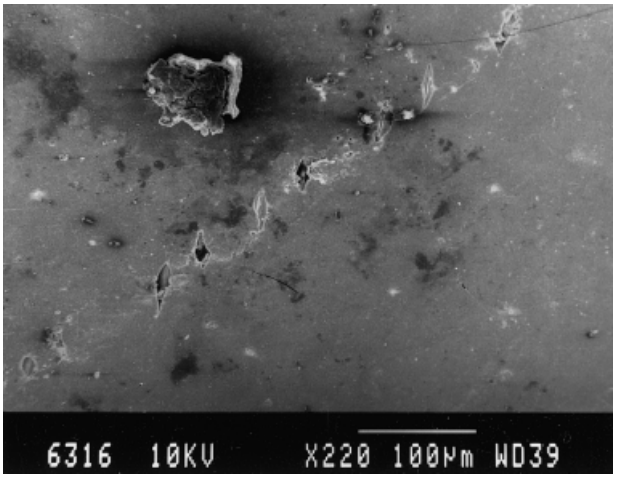

Figure 8 SEM micrograph showing the origin of cracks at the filler particle.

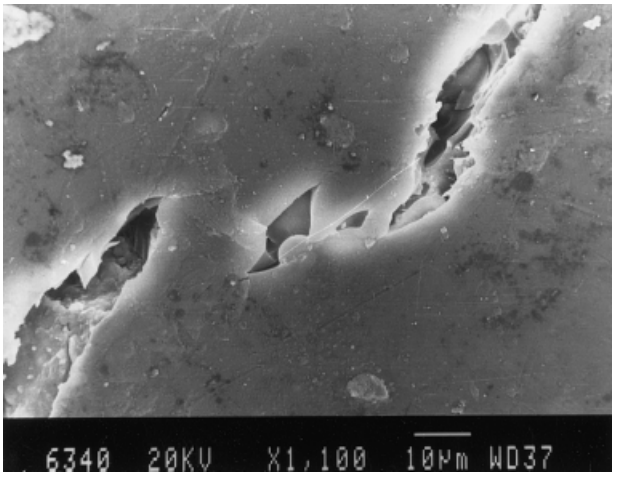

Figure 9 SEM micrograph showing the position of the grown cracks prior to a phase where joining of defects can occur.

emphasized earlier. To explain the difference in values noted for the case of the sample with 30% volume fraction of filler, the tendency for the filler particles to form clusters [Fig. 5(c)] could be invoked. Such clusters favor formation of voids whose presence facilitate the early failure of the test coupon, with a significant reduction in both strength and modulus values.

CONCLUSIONS

- Fly ash, when used as filler in epoxy, brings about an improvement in composite proper-

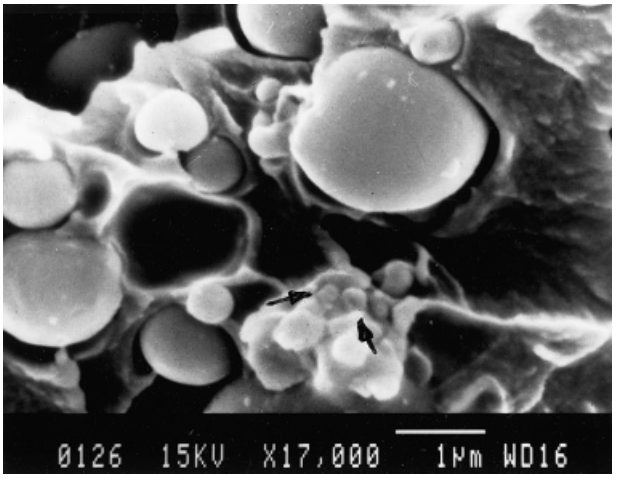

Figure 10 Crescent-shape debonds around larger particles and their lesser formation at smaller particles (indicated by arrows).

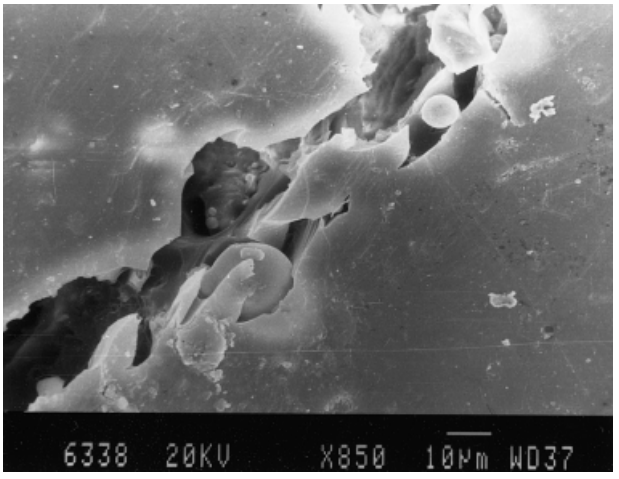

Figure 11 Full-grown crack with two fly ash particles visible.

ties. However, when added beyond 10%, the strength of the composite decreases because of the interaction of debonds at the filler–matrix interface.

- Strength and the modulus values registered at maximum relative packing volume studied (0.36) are significantly lower. The reason for this may be attributed to the tendency of the particles to cluster at higher concentrations. The experimental values of strength and modulus are generally found to match well with those predicted by the rule of mixtures.
- The strengthening effect at lower concentrations is attributed to the widely spread particles interacting less as a result of their large interparticle distances.
- Cracks are initiated at debonds in the opening mode, and the trend to joining of such cracks is unambiguously illustrated in the SEM study of compression surfaces of the failed sample.
- This joining of growing defects is augmented when decreased interparticle distances at higher volume fractions of filler are encountered. All these interactions effectively lower both strength and modulus values of the system.

The authors thank Mr. Sasidhara, Mr. Gurulinga, and Mr. Molliah of the Department of Metallurgy for the help rendered by them during testing and inspection of the samples and also in the preparation of this manuscript. The first author (S.M.K.) expresses his gratitude to colleagues in Civil Engineering for their help in acquiring and characterizing the fly ash.

REFERENCES

1. Pukanszky, B.; Tudos, F.; Jancar, J.; Kolarik, J. J Mater Sci 1989, 8, 1040.
2. Xavier, S. F.; Shultz, J. M.; Friedrich, K. J Mater Sci 1990, 25, 2411.
3. Xavier, S. F.; Shultz, J. M.; Friedrich, K. J Mater Sci 1990, 25, 2421.
4. Xavier, S. F.; Shultz, J. M.; Friedrich, K. J Mater Sci 1990, 25, 2428.
5. Mareri, P.; Bastide, S.; Binda, N.; Crespy, A. Compos Sci Technol 1998, 58, 747.
6. Jarvela, P. A.; Jarvela, P. K. J Mater Sci 1996, 31, 3853.
7. Vollenberg, P. H. Th.; Heikens, D. J Mater Sci 1990, 25, 3089.
8. Rusu, M.; Sofian, N.; Rusu, D. Polym Test 2001, 20, 409.
9. Barta, S.; Bielek, J.; Dieska, P. J Appl Polym Sci 1997, 64, 1525.
10. Brito, Z.; Sanchez, G. Compos Struct 2000, 48, 79.
11. Hussain, M.; Nakagira, A.; Nishijima, S.; Niihara, K. Mater Lett 1996, 27, 21.
12. Chand, N. J Mater Sci Lett 1988, 7, 36.
13. Saroja devi, M.; Murugesan, V.; Rengaraj, K.; Anand, P. J Appl Polym Sci 1998, 69, 1385.
14. Wong, K. W. Y.; Truss, R. W. Compos Sci Technol 1994, 52, 361.
15. Srivastava, V. K.; Shembekar, P. S. J Mater Sci 1990, 25, 3513.
16. Pedlow, J. W. in Coal Ash Utilization Fly Ash, Bottom Ash and Slag; Torrey, S., Ed.; Noyes: Park Ridge, NJ, 1978; p 353.
17. Ferrigno, T. H. in Handbook of Fillers and Reinforcements for Plastics; Katz, H. S.; Milewski, J. V., Eds., Van Nostrand Reinhold: New York, 1978; p 29.
18. Gao, Z.; Tsou, A. H. J Polym Sci Part B: Polym Phys 1999, 37, 155.
19. Zallen, R. Physics of Amorphous Solids; Wiley: New York, 1978; p 183.
20. Milewski, J. V. in Handbook of Fillers and Reinforcements for Plastics; Katz, H. S.; Milewski, J. V., Eds.; Van Nostrand Reinhold: New York, 1978; p 66.
21. He, D.; Jiang, B. J Appl Polym Sci 1993, 49, 617.